Table 2 *Tyrosine hydroxylase and dopamine β-hydroxylase activities of rat heart during postnatal development and ageing.*

Age	No. of rats	TH specific activity (n mol DOPA/mg protein/15 min.)	DBH specific activity (n mol octopamine/ mg protein/30 min.)
1 day	12	0.625 ±0.04	30.75 ±2.2
15 days	8	0.792 ±0 05	37.21 ±2.7
30 days	8	1.562 ±0.08	41.70 ±5.2
3 months	8	1.729 ±0.11	54.93 ±2.9
1 year	6	0.868 ±0.09	38.33 ±1.3
2 years	6	0.663 ±0.09	33.35 ±4.5

Values are mean ± S E., $P < 0.01$.

respect to age. Changes in biogenic amine levels of rat brain during development and ageing has been reported by several workers[10,11]. Catecholamine biosynthesis is regulated by the activity of TH, and possibly in the case of NE, also by the activity of DBH. It is likely that the effect of development and ageing on catecholamine biosynthesis may be due to a change in the catalytic property or in the concentrations of these enzymes. The activity in human serum was reported to increase markedly for the first 2–3 years attaining maximum constant level during adulthood[12]. A decrease in TH activity in aged rats were reported by few workers[13,14]. Implication of metabolizing enzymes monoamineoxidase[15] and catechol-o-methyltransferase[16] in the regulation of catecholamine levels can not be ruled out since the activities of these enzymes has been reported to increase in the brain of senescent rats. The findings suggest that biosynthetic enzyme activities and catecholamine levels are impaired in ageing rats. The biosynthetic enzymes play an important role in regulation and control of catecholamine levels during development and ageing.

Financial assistance by CSIR, New Delhi, to MS is acknowledged.

2 August 1983; Revised 2 January 1984

1. Srivastava, M. and Kapoor, N. K., *Indian J. Exp. Biol.*, 1979, **17,** 1413.
2. Finch, C. E., Foster, J. R. and Mirsky, A. E., *J. Gen. Physiol.*, 1969, **54,** 690.
3. Goodrick, C. L., *J. Gerontol.*, 1971, **26,** 58.
4. Barbeau, A., *J. Am. Geriatr. Soc.*, 1973, **21,** 145.
5. Samorajski, T., Rolsten, C. and Ordy, J. M., *J. Gerontol.*, 1971, **26,** 168.
6. Nagatsu, T. and Yamamoto, T., *Experientia*, 1968, **24,** 1183.
7. Nagatsu, T. and Udenfriend, S., *Clin. Chem.*, 1972, **18,** 980.
8. Srivastava, M. and Kapoor, N. K., *Indian J. Exp. Biol.* 1980, **18,** 647.
9. Srivastava, M. and Kapoor, N. K., *J. Biosci.*, 1983, **5,** 261.
10. Coyle, J. T. and Henry, D., *J. Neurochem.*, 1973, **21,** 61.
11. Bennett, D. and Giarman, N., *J. Neurochem.*, 1965, **12,** 911.
12. Freedman, L. S., Ohuchi, T., Goldstein, M., Axelrod, F., Fish, I. and Dancis, J., *Nature (London)*, 1972, **236,** 310.
13. McGeer, E. G., Fibiger, H. C., McGeer, P. L. and Wickson, V. *Exp. Gerontol.*, 1971, **6,** 391.
14. Algeri, S., Bonati, M., Brunello, N., Ponzio, F., Stramentinoli, G. and Gualane, M., In *Proc. 10th CINP Congress*, Quebec, Canada, July, (ed.) D.E. Domino, Pergamon Press, Oxford, 1977.
15. Robinson, D. S., *Fed. Proc.*, 1975, **34,** 103.
16. Stramentionoli, G., Gualano, M., Catto, E. and Algeri, S., *J. Gerontol.*, 1977, **34,** 392.

SPECTRAL INTERPRETATION OF SELF-POTENTIAL ANOMALY DUE TO AN INCLINED SHEET

S. V. SESHAGIRI RAO and N. L. MOHAN
Centre of Exploration Geophysics, Osmania University, Hyderabad 500 007, India.

THE self-potential method is one of the simplest techniques of prospecting geophysics for the exploration of metallic sulphides and some other conductive

deposits. Paul[1] formulated computer oriented method that depends on successive approximations. Though the application of frequency analysis has radically changed the quantitative interpretation of gravity and magnetic data[2,3], very little has been done in the field of electrical data.

In the present communication an attempt is made to investigate the applicability of the Fourier transformation for the analysis of self-potential data. The causative body is taken to be an inclined sheet of infinite horizontal extension. The Fourier transform of the self-potential effect of such a body is obtained. The resulting Fourier spectrum is analysed for extracting the body parameters-depth to the centre, width and inclination. The applicability of the method is tested on a synthetic model.

Fourier Transform of the Self-Potential effect:

Consider a sheet of inclination α with the horizontal and extending infinitely in Y-direction. The sheet meets the X–Z plane at the points $(a\cos\alpha, a\sin\alpha)$ and $(-a\cos\alpha, -a\sin\alpha)$ respectively (figure 1). Consider two line poles with linear current densities $-I$ and $+I$ situated on the body in the neighbourhood of the upper end and the lower end respectively. The potential due to the pair of line poles at any point on the free surface is[1]:

$$V(x) = \rho I/2\pi\left[\ln\{(x-a\cos\alpha)^2+(H-a\sin\alpha)^2\} - \ln\{(x+a\cos\alpha)^2+(H+a\sin\alpha)^2\}\right] \quad (1)$$

where ρ is the resistivity of the surrounding medium, a is the half width of the sheet, H is the depth to the midpoint of the width of the sheet.

The Fourier transform of the function $V(x)$ is given by

$$\tilde{V}(\omega) = \int_{-\infty}^{\infty} V(x)\exp(-i\omega x)\,dx \quad (2)$$

where ω is the frequency in cycles per unit distance.

Using (1) and (2) we obtain the real component of $\tilde{V}(\omega)$ as;

$$R(\omega) = \frac{2\rho I}{\omega}\cos(\omega a\,\mathrm{coS}\,\alpha)\cdot \sinh(\omega a\sin\alpha)\exp(-\omega H) \quad (3)$$

Analysis of the Fourier Spectrum:

It is evident from (3) that

$$\lim_{\omega\to 0} R(\omega) = 2I\rho a\sin\alpha \quad (4)$$

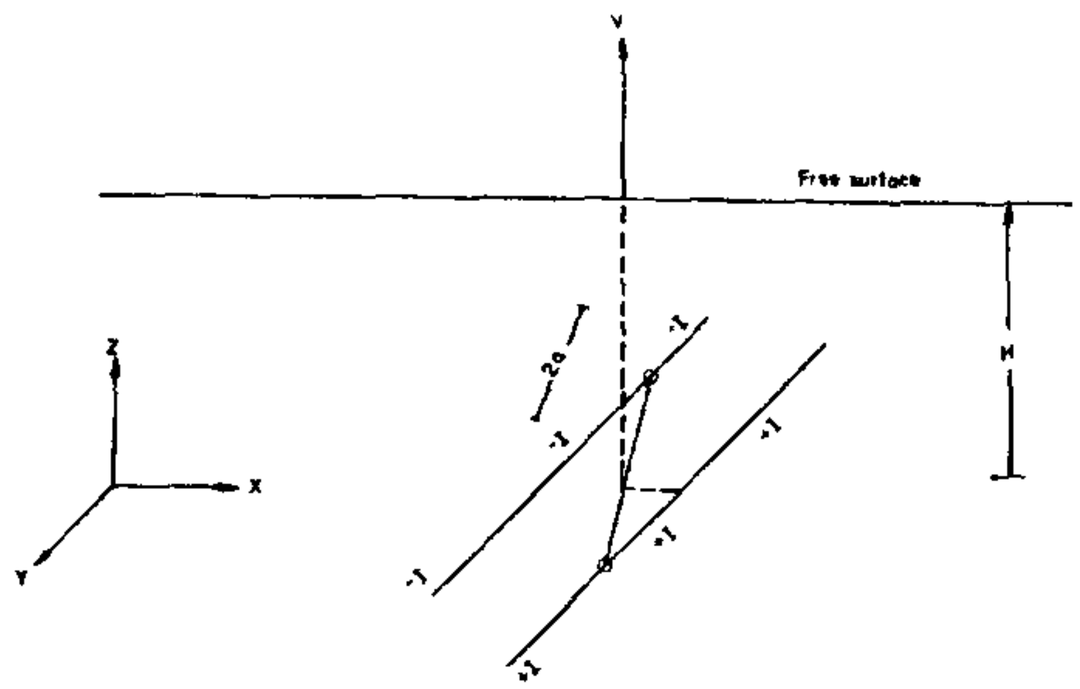

Figure 1. The polarised inclined sheet of infinite horizontal extension.

By virtue of (3) if $\alpha \neq 0$, the $R(\omega)$ vanishes only if

$$\omega_n a\cos\alpha = (2n-1)\frac{\pi}{2} \quad n = 1, 2, 3, \ldots. \quad (5)$$

In particular we write, at $\omega = \omega_1$

$$\omega_1 a\cos\alpha = \frac{\pi}{2}$$

or

$$a\cos\alpha = \frac{\pi}{2\omega_1}. \quad (6)$$

Using (4) and (6) we obtain

$$\alpha = \tan^{-1}\left[\left(\frac{\lim_{\omega\to 0} R(\omega)}{\rho I}\right)\frac{\omega_1}{\pi}\right] \quad (7)$$

Thus (7) facilitates the determination of the parameter α provided ρI is known.

Again from (4) and (6) we get

$$a = \sqrt{\frac{\pi}{4\omega_1^2} + \frac{\left[\lim_{\omega\to 0} R(\omega)\right]^2}{4\rho^2 I^2}}. \quad (8)$$

From (3) we write

$$\exp(-\omega H) = \frac{\omega R(\omega)}{2I\rho\cos(\omega a\cos\alpha)\cdot\sinh(\omega a\sin\alpha)} \quad (9)$$

Denoting the right hand side by $R'(\omega)$ and differentiating with respect to ω we get

$$\frac{d(\ln[R'(\omega)])}{d\omega} = -H \quad (10)$$

Application:

In order to test the procedure outlined above for determining the body parameters, we consider a synthetic model assuming $\rho I = 1$ unit. Model parameters are given in the table 1.

Table 1 *Synthetic models of the inclined sheet.*

Parameters	α in degrees	a† units of length	H† units of length
Assumed	60°	2	5
Evaluated	53° 09′	1.83	4.77

† In arbitrary units.

The self-potential effect due to inclined sheet of infinite horizontal extension is computed with the help of (1) and are shown in figure 2. The real component of the Fourier transform of the self-potential effect is calculated from (3) and shown in figure 3. Since the field data is always discrete but not a continuous estimate, in order to facilitate the vertication of the present method we digitise the self-potential effect of the model at an interval of 0.1 units.

The real part of the discrete Fourier transform of the self-potential effect $V(x)$ is given by:

$$R(n\omega_0) = \sum_{l=0}^{N-1} V(l \cdot \Delta x) \cos(n\omega_0 \cdot l\Delta x) \qquad (11)$$

where $\omega_0 = 2\pi/N \cdot \Delta x$ is the fundamental frequency, N is the number of points and Δx is the sample interval. In the present case $\Delta x = 0.1$ units, $N = 512$ and ω_0 $= 2\pi/(512 \times 0.1)$ radians per unit length. The graph of $R(n\omega_0)$ *vs* $n\omega_0$ is shown in figure 4. Using this graph and (7) and (8) we obtained the values of α and a. Subsequently H is obtained from the plot of $\ln[R'(n\omega_0)]$ *vs* $n\omega_0$ (figure 5). The evaluated values are

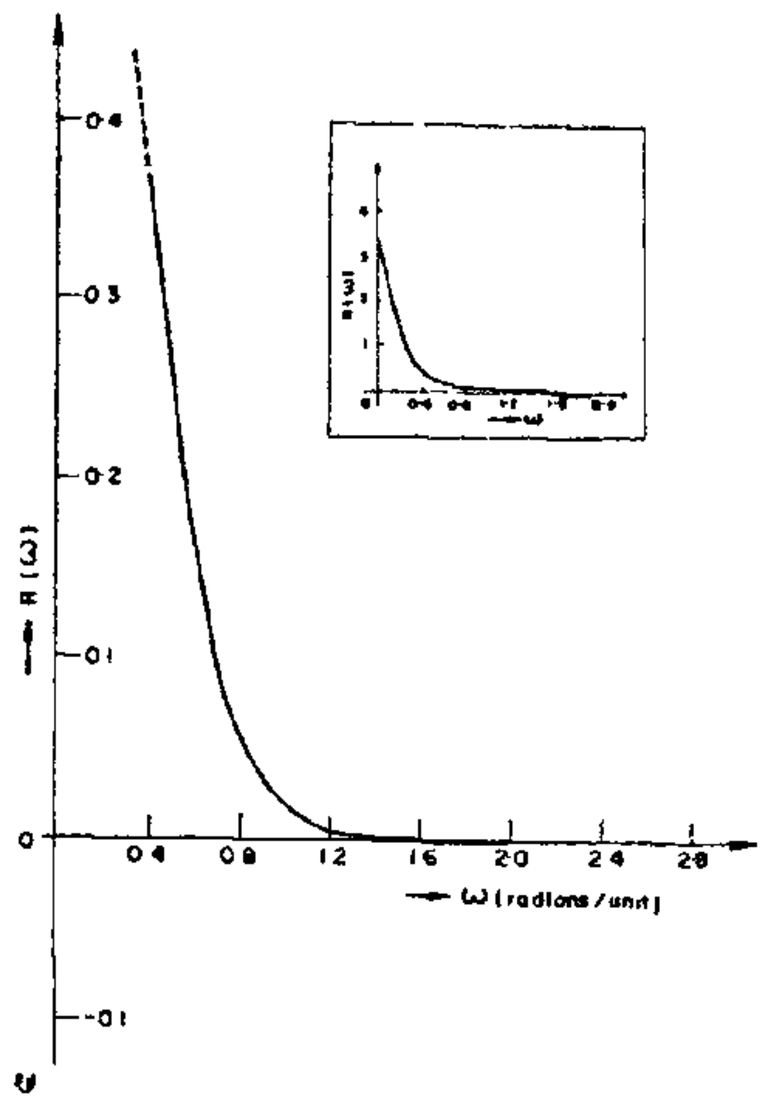

Figure 3. Computed $R(\omega)$ *vs* ω of the self-potential effect.

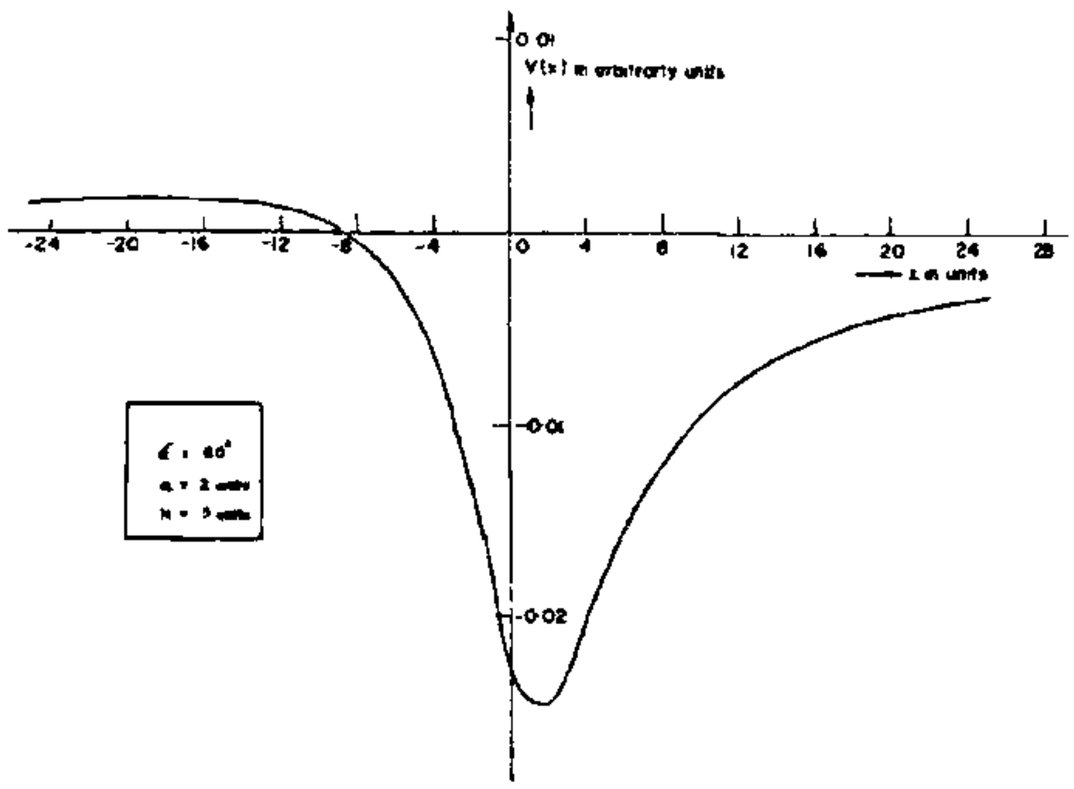

Figure 2. Computed self-potential anomalies due to an inclined sheet of infinite horizontal extension.

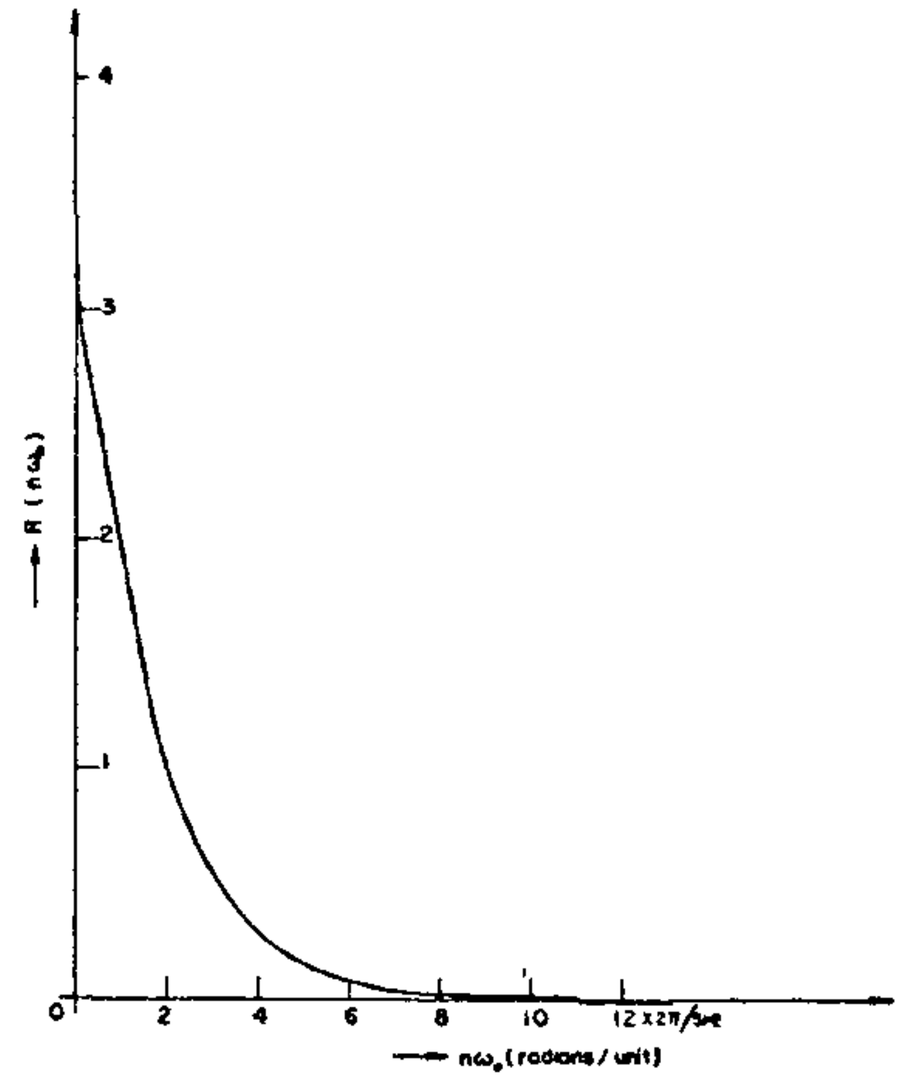

Figure 4. Graph of $R(n\omega_0)$ *vs* $n\omega_0$ of the self-potential effect.

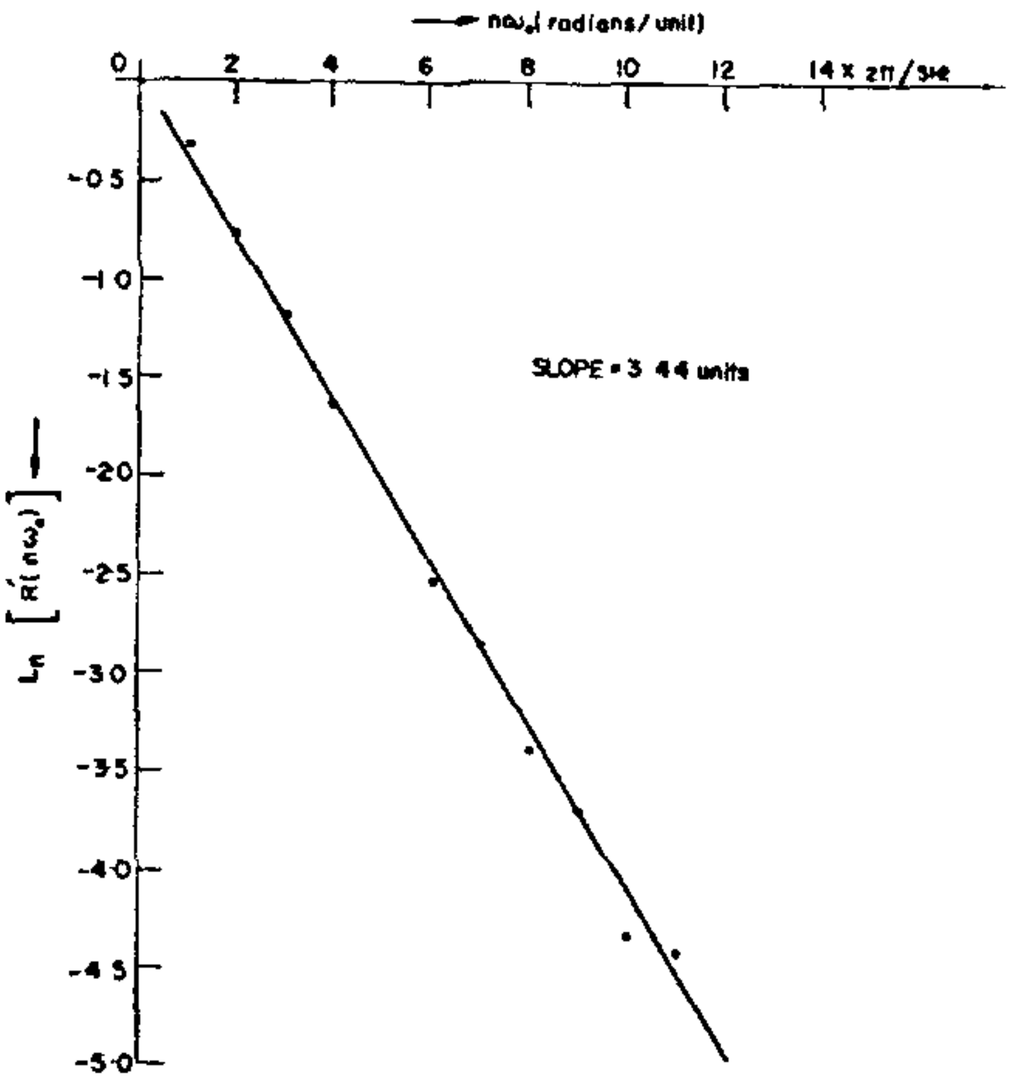

Figure 5. Graph of $\ln[R'(n\omega_0)]$ *vs* $n\omega_0$.

given in table 1. The tabulated values establish the validity of the technique. It may be observed that on an average the error does not exceed 8.2 %.

21 February 1983

1. Paul, M. K., *Geophysics*, 1965, **30**, 418.
2. Odegard, M. E. and Berg, Jr. J. W., *Geophysics*, 1965, **30**, 424.
3. Bhimasankaram, V. L. S., Mohan, N. L. and Seshagiri Rao, S. V., *Geoexploration*, 1978, **6**, 259.

Ru(III) CATALYSED OXIDATION OF 1,3 BUTANDIOL BY PHENYLIODOSOACETATE. A KINETIC STUDY

SUBAS C. PATI and BIKASH R. DEV*
Department of Chemistry, Berhampur University, Berhampur 760 007, India.
**Department of Chemistry, Godavaris Mahavidyalaya, Banpur 752 031, India.*

Diols have been subjected to oxidation by various oxidising agents both in the presence and absence of catalyst[1-3]. In continuation of our earlier work[4-6], We report in this present communication, some interesting results of Ru(III) catalysed oxidation of 1,3 butandiol by phenyliodosoacetate (PIA).

All the chemicals were of BDH (AR) grade. Phenyliodoso-acetate (PIA) was prepared by the modified method of Boesken and Schneider[7]. Ru(III) chloride (Johnson Mathey, London) was standardized by the method of Horiuchi *et al*[8]. The progress of the reaction was monitored by estimating PIA at regular intervals of time iodometrically. The product in the case of 1,3 butandiol is identified to be 3-hydroxy butanal, confirmed from its hydrazone derivatives.[9]

Interestingly the kinetic orders in the case of 1,3 butandiol are strikingly different from those of other diols studied[6]. The reaction in the case of 1,3 butandiol is found to be first order in the oxidant as evident from a good linearity in the plot of log (PIA) versus time upto 75% of reaction. The pseudo-first order rate constant K_{obs} is also found to be constant over a wide range of PIA concentration (table 1), whereas earlier we have observed a zero order dependence on oxidant in the Ru(III) catalysed oxidation of diols (ethyleneglycol, 1,2 propandiol and 1,4 butandiol) by phenyliodosoacetate[6].

Table 1 *Effect of varying [Oxidant]/[Substrate] on the reaction rate:*

$[HClO_4] = 0.01$ M, HOAc = 10% (v/v), $[Ru(III)] = 8.87 \times 10^{-7}$ M, Temp. = 35°C.

10^3 [PIA] M	10^4 [S] M	10^3 k_1 min^{-1}
0.222	10.0	44.47
0.462	10.0	42.77
0.733	10.0	44.51
1.000	10.0	43.10
1.53	10.0	44.50
0.50	5.00	42.97
0.50	10.02	42.77
0.50	20.04	44.59
0.50	50.10	42.75

A ten fold increase in the concentration of 1,3 butandiol does not affect the pseudo-first order rate constant (table 1), proving the order with respect to substrate to be zero, whereas a first order dependence on (substrate) has been observed by us in the Ru(III) catalysed oxidation of diols by phenyliodosoacetate[6].

The pseudo-first order rate constants increase on increasing the concentration of Ru(III) (table 2). The plots of log k_{obs} versus log [Ru(III)] are linear with unit slopes. The effect of $HClO_4$ on the reaction rate is found to be independent (table 2). An increase in the